* Micromechanical Structures and Microelectronics for Acceleration Sensing

^ Brady R. Davies, Stephen Montague, James H. Smith, Mark Lemkin

Intelligent Micromachine Department
Sandia National Laboratories, P.O. Box 5800 MS 1080
Albuquerque, New Mexico 87185-1080
http://www.mdl.sandia.gov/Micromachine

ABSTRACT

MEMS is an enabling technology that may provide low-cost devices capable of sensing motion in a reliable and accurate manner. This paper describes work in MEMS accelerometer development at Sandia National Laboratories. This work leverages a process for integrating both the micromechanical structures and microelectronics circuitry of a MEMS accelerometer on the same chip. The design and test results of an integrated MEMS high-g accelerometer will be detailed. Additionally a design for a high-g fuse component (low-G or ≈ 25 G accelerometer) will be discussed in the paper (where 1 G ≈ 9.81 m/s).

In particular, a design team at Sandia was assembled to develop a new micromachined silicon accelerometer which would be capable of surviving and measuring high-g shocks. Such a sensor is designed to be cheaper and more reliable than currently available sensors. A promising design for a suspended plate mass sensor was developed and the details of that design along with test data will be documented in the paper. Future development in this area at Sandia will focus on implementing accelerometers capable of measuring 200 kilo-g accelerations. Accelerometer development at Sandia will also focus on multi-axis acceleration measurement with integrated microelectronics.

Keywords: micromachined sensors, capacitive sensors, accelerometer

2.0 INTRODUCTION

The acceleration environment experienced by the sensors and electronics in an earth-penetrator weapon is extreme, with average accelerations in the 20,000-G range and peak transient accelerations up to several hundred thousand G's. Earth penetrators often contact earth, concrete, rocks, or other hard materials while traveling at thousands of feet per second. Sensors must be able to survive both penetrator launch as well as contact and penetration while distinguishing between each. Commercially available accelerometers used in shock testing of earth-penetrator weapons components are both expensive ($1800 each) and prone to failure.

Commercially available accelerometers tend to fail due to lack of damping and breaking packaging leads. The only reported silicon-based high-G accelerometers are bulk-micromachined[1]. Preliminary failure analysis of these commercial sensors indicated that failure modes included both undamped high-frequency resonances of the sensor itself and catastrophic failure of the packaging.

---

* This work was supported by the United States Department of Energy under Contract DE-AC04-94AL85000. Sandia is a multiprogram laboratory operated by Sandia Corporation, a Lockheed Martin Company, for the United States Department of Energy.

^ B.R.D. (correspondence): Email: brdavie@sandia.gov; Telephone: (505) 844-5600
S.M. (correspondence): Email: smonta@sandia.gov; Telephone: (505) 844-6954
J.H.S. (correspondence): Email: smithjh@sandia.gov; Telephone: (505) 844-3098
M.L. Berkeley Sensor and Actuator Center

Designs for suspended high-G and low-G plate mass sensors were developed and will be described in this paper. The high-G sensor design was developed to directly measure acceleration and shock during earth-penetrator operation. The low-G sensor design was developed to begin coupling multiple fuse functions into a single, integrated device in order to reduce size, power, and cost while increasing reliability and performance.

3.0 INTEGRATED SUSPENDED MASS HIGH-G ACCELEROMETER DESIGN

A suspended mass, high-G accelerometer was designed and fabricated in a variation of Sandia's integrated surface-micromachined polysilicon / electronics manufacturing process[2]. This sensor consists of a parallel-plate capacitor, with one plate stationary with respect to the sensor housing and the second plate suspended by flexible beams that deflect in proportion to the magnitude of the acceleration imposed upon the sensor housing. The sensor was designed to measure accelerations up to 50 kilo-G with a resolution of 50 G. Dominant design tradeoffs include balancing sufficient plate deflections sufficient to obtain acceptable signal-to-noise ratios from the capacitive sensors against stiff mass suspension elements necessary to obtain responsive sensor measurements (high bandwidth). Additional design tradeoffs include optimizing response by designing a critically damped system subject to processing constraints. This design takes advantage of Sandia's new integrated surface-micromachining/CMOS manufacturing process to incorporate the capacitive pick-off electronics on-chip. Additionally, multiple sensors were fabricated together on the same chip, so that multiple sensors could be tested with a single shock, and the sensors could be readily used in a redundant, fault-tolerant architecture.

The mechanical elements of the high-G accelerometer were fabricated using two layers of polycrystalline silicon with a separation of two microns. The upper layer contains the moving mechanical element of the sensor, and the bottom layer acts as both a structural and electrical ground. The sensor principle of operation is to measure capacitance changes between the two plates with CMOS electronics located adjacent to the mechanical elements (same substrate).

3.1 High-G accelerometer specifications

Nominal parallel-plate capacitance for the 50 kilo-G sensor is 100 fF at a 2 μm gap. This capacitance level is constrained by the necessity to interface with an existing CMOS microelectronics design. When no acceleration was applied to the sensor, its nominal capacitance requirement constrained both the gap spacing and plate overlap area. This translated into a plate overlap area of $\cong$ 22, 500 μm^2 ($\cong$ 150 μm x 150 μm square area), where the no acceleration gap spacing was constrained by the 2 μm thick sacrificial oxide layer used in the fabrication process. The desired gap spacing during acceleration of 50 kilo-G is 1 μm. The resonant frequency of the sensor suspension is constrained to be greater than 100 kHz to accommodate sampling frequencies and the induced vibration caused by the sampling voltage electrostatic attractive force. To obtain adequate response,a target range of 0.4 to 0.6 for the damping ratio is also desired. This range was principally dictated by fabrication considerations, specifically the requirement for sufficient spacing of etch- release holes. In this case, there is very little design flexibility to control damping.

3.2 High-G accelerometer mechanical design

The first prototype suspended mass sensor consists of fourteen beam elements (seven on each side) that act as springs to cantilever a 22,600 μm^2 plate mass (top layer of polycrystalline silicon) over a bottom electrode (bottom layer of polycrystalline silicon). A top view of the sensor and reference capacitor is shown in Figure 1. The sensor consists of two plate masses, one of which serves as a reference capacitor during acceleration measurements. The sensor element on the right is suspended by 14 beams, each 7 μm x 90 μm in size. Each beam acts as a spring allowing the square plate mass in the center of the sensor to move up or down. The reference capacitor, on the left, is a parallel plate capacitor identical in geometry to the sensor parallel plate capacitor with the exception of spring elements. Spring elements in the reference capacitor are designed to be very stiff, so that at the acceleration levels relevant to sensor operation, the spring elements permit negligible deflection of the plate mass. The reference capacitance and sensor capacitance are compared electronically to measure acceleration.

Each suspended mass is perforated by 324, 2μm x 2μm etch-release holes. The number and spacing of the etch-release holes (necessary for proper fabrication of the sensor element) results in a damping ratio at 50 kilo-G of acceleration of $\cong$ 0.4. The

calculated natural frequency of the sensor is ≅ 127 kHz with a damped natural frequency of ≅ 118 kHz. Cross-axis sensitivity should be minimal and the fracture factor of safety of the device was calculated to be almost three. Results of testing the suspended mass prototype sensor are included in section 3.4 of this paper.

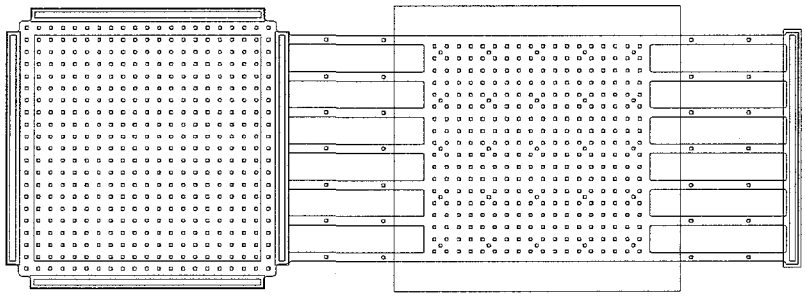

Reference Capacitor **Sensor**

Figure 1: First prototype suspended mass sensor and reference capacitor top view

Damping was determined by simultaneously applying three different models of squeeze film damping, each of which models some but not all of the applicable characteristics of the suspended mass prototype. Squeeze-film damping can be defined as the viscous loss of energy due to pumping a viscous fluid out from or into the volume between two moving surfaces.

The first model[3] is applicable to squeeze-film damping between two parallel disks without perforations that are separated by several microns. In this model, viscous damping occurs due to the movement of fluid around the outside edges of the plates. The damping resistance, R_{film}, is characterized by the following equation:

$$R_{film} = 3\mu S^2/2\pi\delta^3 \ \text{(N-s/m)} \qquad (1)$$

where μ is the fluid viscosity (18×10^{-6} kg/m-s for air at 20 °C), S the plate area overlap, and δ the average plate spacing.

The second model[3] is applicable to squeeze-film damping when one plate is perforated. In this model, viscous damping occurs due to the flow of fluid through the perforations. The damping resistance, R_{perf}, is characterized by the following equation:

$$R_{perf} = 12\mu S^2/N\pi\delta^3 G(A) \ \text{(N-s/m)} \qquad (2)$$

where A is the fraction of open area in the plate, and N is the total number of holes in the perforated plate. The function G(A) is described in equation (3).

$$G(A) = [A/2 - A^2/8 - (\ln A)/4 - 3/8] \qquad (3)$$

The third model[3] is applicable to squeeze-film damping at high frequencies (> 10 kHz). This viscous resistance is called radiation resistance and is characterized by the following equation:

$$R_{rad} = \rho c(A\omega/c)^2 \qquad \text{(N-s/m)} \qquad (4)$$

where ρ and c are the density and speed of sound of the viscous fluid, and ω is the motion frequency. Each of the three models was applied to the design of the suspended mass accelerometer by modeling each of their respective damping contributions and combining them as parallel elements (as shown in Figure 2).

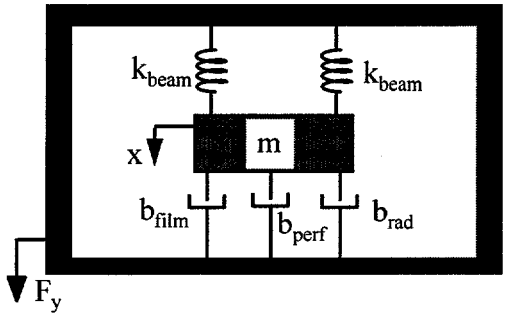

Figure 2: Schematic model for suspended mass accelerometer mechanical elements

3.3. High-G Accelerometer Electrical design

The CMOS circuit for the high-G accelerometer consists of a unity gain buffer followed by a gain stage and output driver. The purpose of the circuit is to measure the change in capacitance of the sensor capacitor relative to the fixed reference capacitor. The sensor capacitor and the reference capacitor are connected in series and an AC signal (100 kHz, ± 5 V P-P) is applied across the pair. If the two capacitors are not equal, an output signal appears at the common node of the pair. This signal is proportional to the acceleration and is sensed by the CMOS circuit.

Since the sensor capacitors are small, the input capacitance of the circuit is also very small. The first stage consists of an n-channel source follower by an input capacitance of $\cong$ 40 fF. Noise limits the sensitivity of the circuit, so the circuit was designed to have an input noise of less than $2\mu V/Hz^{1/2}$. The second stage is a combination gain stage and output driver. The gain is $\cong$ 100 and the output driver is designed to be compatible with the off-chip loads.

Integrating the CMOS electronics on the same substrate as the micromachines enables the microelectronics to measure extremely small capacitance changes (on the order of fractions of atto Farads). This enables the sensor to be operated over a high dynamic range and still measure relatively small changes in acceleration. Additionally, parasitic noise is reduced while bandwidth is increased in the integrated electronics configuration.

3.4 High-G Accelerometer Test Results

Preliminary test results for the first suspended mass accelerometer prototype demonstrated reasonable correlation between acceleration levels and sensor output at G levels under 15 kilo-G (6 kilo-G, 10 kilo-G, and 14 kilo-G). At higher G levels (above 16 kilo-G), sensor output was saturated and so could not be correlated to acceleration level.

The suspended mass accelerometer output signals also appeared to contain carrier signal components, shock signal artifacts, and unidirectional output bias. A filtered sample test trace is included in Figure 3. A number of electronic as well as mechanical issues that likely contributed to the sensors' operation were identified and addressed. These issues included residual stress in the suspended mass suspension, resonant overtravel, output bias, underdamped mass motion, output amplifier saturation, excessive design gain, and incomplete comparator signal cancellation.

4.0 REVISED HIGH-G ACCLEROMETER DESIGN

Two different revised mechanical designs were developed and are currently being fabricated using the Sandia integrated process. The first revised mechanical design is shown in Figure 4. In this design, the suspension system was modified to incorporate greater compliance in both the vertical and horizontal directions. The additional vertical compliance was added to enable increased movement of the plate mass in the sensing direction. The additional horizontal compliance was added to relieve any residual stress that might remain in the structural polycrystalline silicon after processing. The bent beams provide stress relief in the horizontal plane. Both the mechanical design and CMOS circuit design used in the first suspended mass prototype were enhanced to resolve performance reduction factors identified in the previous section. The revised mechanical element was designed to be compatible with the improved CMOS circuitry.

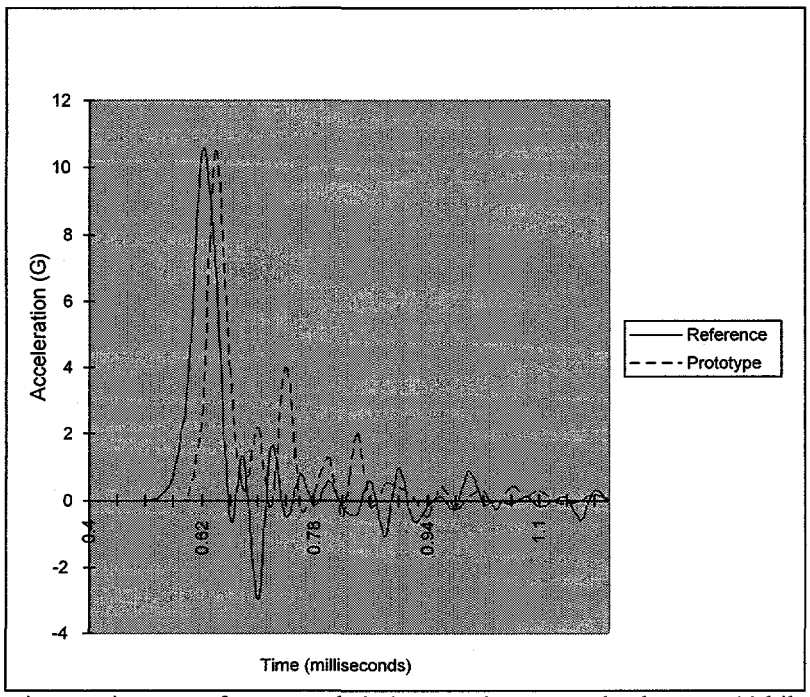

Figure 3: Filtered acceleration vs. time trace for suspended plate accelerometer shock test at 10 kilo-G

An additional mechanical design was developed to be compatible with a new CMOS sensing circuit. Both the electronic circuitry and the mechanical design were based on an inertial sensor designed at the University of California at Berkeley and fabricated at Sandia.[4] Both the electronic and mechanical elements of the Berkeley design were adapted to the high-G acceleration environment. CMOS circuitry compatibility required the use of a sensing mass with a much larger capacitive area (72,900 μm^2 with a nominal capacitance of 325 fF) than was used in the previous accelerometer design.

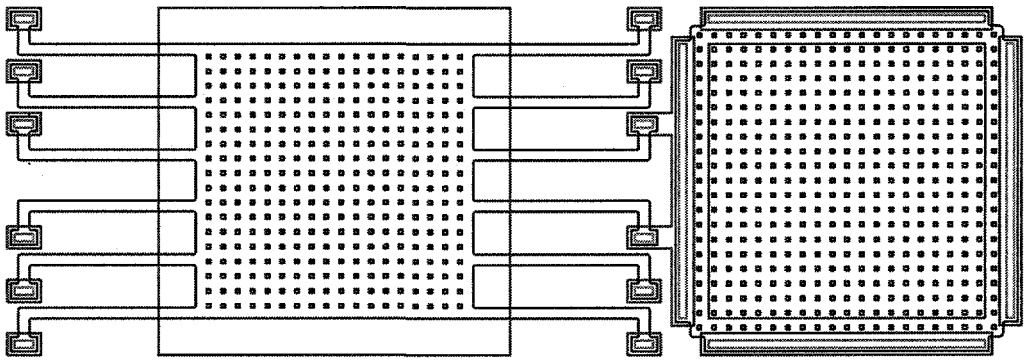

SENSOR **REFERENCE CAPACITOR**

Figure 4: Bent beam mechanical design for high-G accelerometer

4.1 Finite element analysis of the high-G accelerometer bent beam design

Finite element analysis software was used to verify the design of the bent beam high-G accelerometer. The finite element software that was used is called ANSYS/AutoFEA® 3D, and is compatible with AutoCAD® generated geometry. Results of this analysis software predicted somewhat different deflection and resonant frequency values than those obtained through manual analysis. The software predicted that the structure would resonate at 151 kHz as compared to manual analysis resulted in a prediction of 101 kHz (Table 1). The finite element software predicted maximum deflection at 50 KG of 0.64 microns compared to 0.95 microns using manual analysis techniques (Figure 5). Additionally, finite element software

predicted a maximum principal stress level of 93.2 MPa at 50 kilo-G compared to 74 MPa using manual analysis techniques (Table 1).

• Vibration Frequencies:	• Maximum Deflection (@ 50 k-g's):
– Mode 1: 151 kHz	– 0.64 microns
– Mode 2: 240 kHz	• Maximum Stress (@ 50 k-g's):
– Mode 3: 470 kHz	– 93.2 MPa
– Mode 4: 498 kHz	
– Mode 5: 747 kHz	
– Mode 6: 876 kHz	

Table 1: Finite element predictions of frequency modes, maximum deflection and stress of revised high-G accelerometer

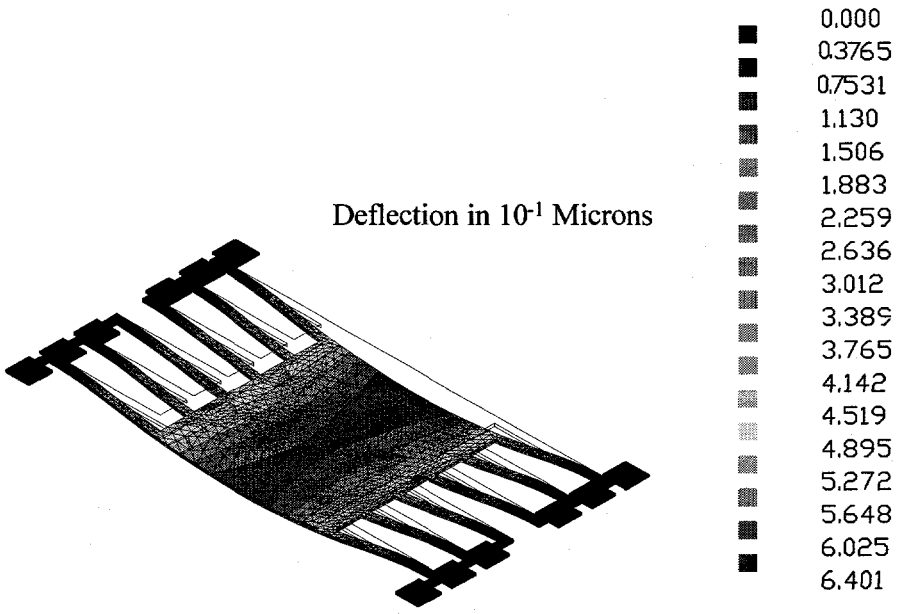

Figure 5: Deflection of revised high-G sensor design at 50 kilo-G

5.0 LOW-G ACCELEROMETER

Both high-G and low-G acceleration sensing are important elements of some fuse applications. High-G accelerometers are necessary for measuring shock levels and discriminating between impact and shock acceleration events. Low-G accelerometers are necessary for such functions as safety, navigation, and condition monitoring. A low-G accelerometer was also designed and will be fabricated using a new microelectronics integrated three-level polycrystalline silicon process recently developed at Sandia. The low-G accelerometer was designed to measure accelerations between ± 25 G's. Design of the mechanical suspension and microelectronics is similar to the high-G accelerometer design with appropriate scaling applied. Additionally, the low-G accelerometer mechanical structure was designed to be controlled using a $\Sigma\Delta$ control system similar to those designed by Lemkin, et. al. at the University of California at Berkeley[4]. The spring suspension system as well as electrostatic electrodes is shown in Figure 6. Mechanical stops were also implemented at each corner and the center of the capacitive plate sensor to restrict lateral and vertical movement during high-G events.

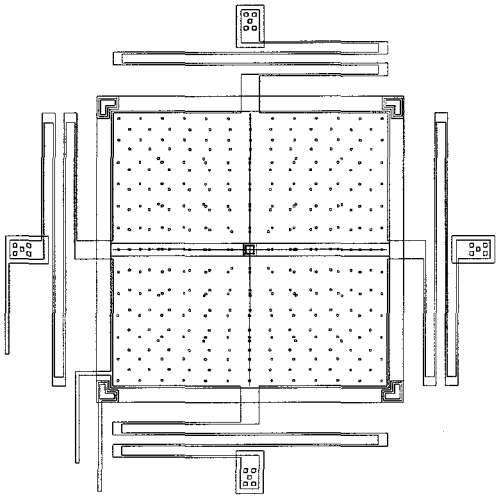

Figure 6: Schematic of low-G accelerometer

5.1 Finite element analysis of the low-G accelerometer

Finite element analysis software was also used to verify the design of the low-G accelerometer. Results of this analysis software predicted maximum deflection at 10 G of 0.15 microns (for the open loop control case) and resonance at 4 kHz (Figure 7 and Table 2). Additionally, the design factor of safety exceeds 10 for the stress states calculated for a 10 G acceleration event.

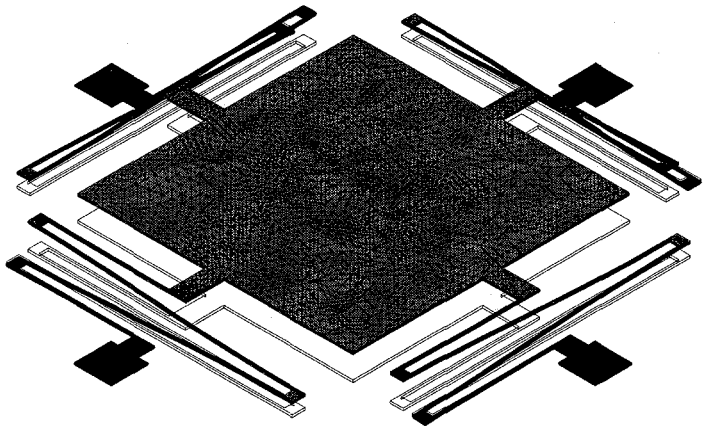

Figure 7: Low-G accelerometer deflection at 10 G

• Vibration Frequencies: – Mode 1: 3,898 Hz – Mode 2: 7,008 Hz – Mode 3: 7,049 Hz – Mode 4: 13,281 Hz – Mode 5: 13,573 Hz – Mode 6: 19,592 Hz	• Maximum Deflection (@ 10 g's): – 0.15 microns • Maximum Stress (@ 10 g's): – 925 KPa

Table 2: Finite element predictions of frequency modes, maximum deflection and stress of low-G accelerometer

6.0 SUMMARY

The first prototype suspended mass high-G accelerometer design showed promising results up to 14 kilo-G, but was not suitable for higher acceleration levels. A second generation series of designs have been developed to improve and correct those factors that contributed to the unsatisfactory performance of the first prototype. These second generation prototypes include two different mechanical designs and three different electronic circuit designs. The second generation prototypes are currently being fabricated and should be ready for testing in the next few months. A low-G accelerometer design has been developed which is compatible with the new integrated microelectronics, three-level polycrystalline silicon process. The low-G accelerometer is suitable for use in a high-G environment as a fuse component.

ACKNOWLEDGMENTS

The authors wish to express their sincere appreciation to The authors wish to express their sincere appreciation to David Ryerson for program direction, Vesta Bateman and Frederick Brown for shock testing, James Murray for CMOS electronics design, Danny Rey for electronics testing, W. Doyle Miller for packaging the sensor, Todd Christenson for leading the failure analysis,, and Tom Gugliotta for fabricating the prototype sensors. Without the outstanding assistance of these dedicated professionals, the work described above could not have been accomplished.

REFERENCES

1. B. R. Davies, et. al., "High-G MEMS Integrated Accelerometer", *SPIE 4th Annual Symposium on Smart Structures and Materials*, March, 1997.
2. J. Smith, S. Montague, J. J. Sniegowski, J. R. Murray, and P. J. McWhorter, "Embedded Micromechanical Devices for the Monolithic Integration of MEMS with CMOS," *IEDM Tech. Digest*, pp. 609-612, Dec. 1995.
3. T. B. Gabrielson, "Mechanical-Thermal Noise in Micromachined Acoustic and Vibration Sensors", *IEEE Transactions on Electron Devices*, Vol. 40, No. 5, May, 1993.
4. M. A. Lemkin, M. A. Ortiz, N. Wongkomet, B. E. Boser, J. Smith, "A 3-Axis Surface Micromachined ΣΔ Accelerometer", *IEEE International Solid-State Circuits Conference*, pp. 202-203, 1997.

DISCLAIMER